*M. R. Bache* and W. J. Evans**

# The Effect of Tension–Torsion Loading on Low Temperature Dwell-Sensitive Fatigue in Titanium Alloys

**REFERENCE** Bache, M. R. and Evans, W. J. **The effect of tension–torsion loading on low temperature dwell-sensitive fatigue in titanium alloys**, *Multiaxial and Fatigue Design*, ESIS 21 (Edited by A. Pineau, G. Cailletaud, and T. C. Lindley) 1996, Mechanical Engineering Publications, London, pp. 229–242.

**ABSTRACT** The paper explores the effect of tension and torsion loading on two near-alpha titanium alloys with grossly different microstructures. The alloy IM1685 is essentially basket-weave with a coarse prior beta grain size of approximately 0.5 mm diameter cross-section. The IMI834 is much finer with a 20–30 $\mu$m structural unit size and consisting of 15 percent primary alpha in a transformed beta matrix. Significantly different behaviour is observed, which can be related to the fact that cracks in IM1685 are small compared with the structural unit, while in IM1834 they are significantly large and have a predominantly Stage II character. The effect of dwell periods at peak stress on the tension and torsion fatigue response is evaluated.

## 1 Introduction

Titanium alloys are used extensively in the aerospace industry for gas turbine disc and blade components. The operating conditions for such applications are demanding and encompass multiaxial, cyclic stress states over a range of temperatures from near ambient up to approximately 600°C. A popular alloy for such use in the 1970s was IM1685 (Ti–6Al–5Zr–0.5Mo–0.2Si), which is a near-alpha titanium alloy developed specifically for its high temperature creep resistance. However, under fatigue a sensitivity to periods of dwell at peak stress was identified for the lower end of the operating temperature range which led to significant reductions in cyclic life. This alloy has since been superseded by other near-alpha variants including IMI834 (Ti–5.8Al–4.0Sn–3.5Zr–0.7Nb–0.5Mo–0.35Si–0.06C), chiefly in response to the need to run engine compressors at higher temperatures. Despite the significant improvements, however, the dwell phenomenon is still a major concern with these newer alloys.

A common characteristic of titanium alloys under fatigue loading is the development of subsurface quasicleavage facets orientated with their basal plane

*IRC in Materials, University of Wales, Swansea, SA2 8PP, UK.

approximately perpendicular to the principal tensile stress. Previous workers have identified an increased tendency for facet formation under dwell and constant load conditions. A number of factors have been invoked to explain facet formation and hence dwell sensitivity, including time-dependent strain accumulation and stress triaxiality. To assess their validity, a programme of work was carried out on the fatigue response of titanium alloys under tension–torsion loading at ambient temperature. The objective was to explore deformation and failure mechanisms under a range of tensile to shear stress ratios for both cyclic and dwell conditions.

## 2 Experimental Methods

### 2.1 *Materials*

Specimens were manufactured from IMI685 and IMI834, both supplied in the form of 30 mm round bar. Prior to machining, IMI685 blanks were heat treated in air above the beta transus (1030°C) for 45 minutes followed by air cooling to laboratory temperature and aging at 550°C for 24 hours. This produced the recommended 'basketweave' microstructure, which consists predominantly of the *widmanstatten* alpha shown in Fig. 1(a) but also contains small regions of aligned alpha plates. The IMI834 was heat treated to give a retained primary alpha content of 15 percent. This was achieved by heating in the alpha + beta field (1025°C) for two hours followed by oil quenching and a two-hour age at 700°C. The 'bi-modal' microstructure shown in Figure 1(b) was obtained.

### 2.2 *Specimen design*

Results presented in this paper were obtained using specimens of two different designs. All torsion testing employed a tubular specimen, Fig. 2(a). CNC machining techniques ensured good axiality and surface finish. The same specimen was used for tension tests on the IMI685 basketweave material. The suitability of this thin-wall specimen for tensile work on this particular alloy and microstructure was confirmed through a solid specimen geometry, Fig. 2(b). This latter design was subsequently adopted for all tension testing on IMI834.

### 2.3 *Test matrix*

A closed-loop servo-hydraulic tension–torsion machine of 50 KN axial load and 400 Nm torque capacity was employed. In the case of IMI685, tests were carried out either under pure tension or torsion at laboratory temperature. For IMI834 an additional in-phase, mixed-mode cycle ($\sigma_{11} = \sigma_{21}$) was investigated. The 'cyclic' and 'dwell' loading waveforms are represented schematically in Fig. 3. Each incorporated a 2-second rise and fall between peak and minimum stress. The one second hold at peak load for cyclic loading was to facilitate data acquisition. Data from the dwell tests were taken shortly before the end of the

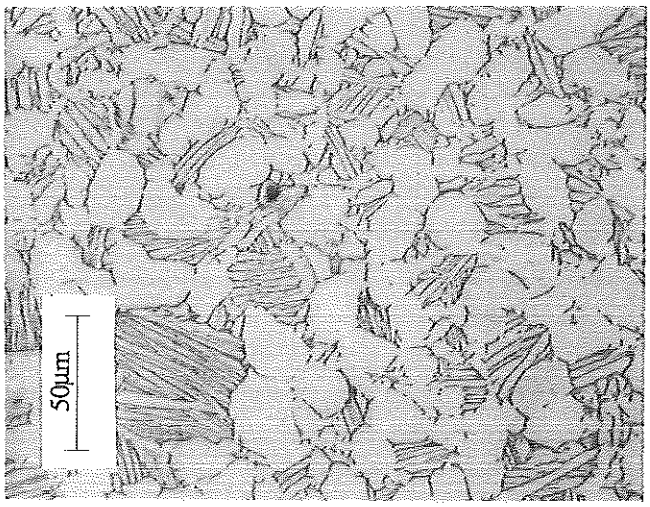


Fig 1(b) Bi-modal IMI834

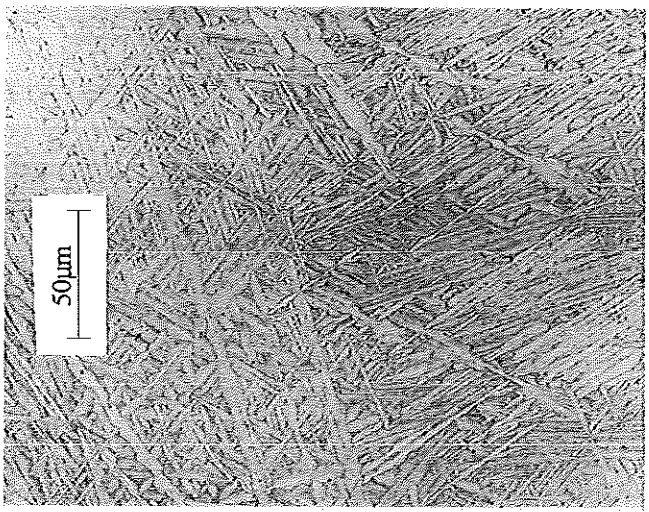


Fig 1(a) Basketweave IMI685

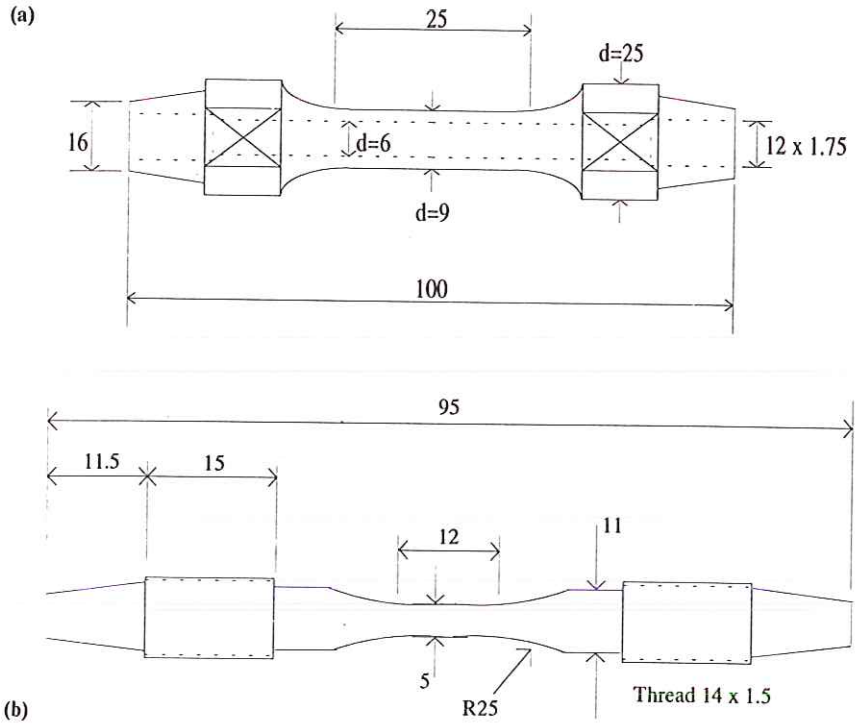


**Fig 2 (a) tubular torsion test piece; (b) solid tensile specimen.**

dwell period. Under all loading configurations an R ratio 0.1 was applied. Extensometry has been developed to monitor axial extension and rotational twist under torsion from the specimen gauge section (1). Tension tests were monitored by means of a commercial strain gauge bridge extensometer. Through the application of in-house software, strain–time records and cyclic life were recorded. Both optical and scanning electron microscopy were used to examine failed specimens.

### 2.4 *Stress and strain criteria*

A modified version of the von Mises stress and strain criteria has been employed in previous papers by the present authors to correlate multiaxial fatigue data (1). The equations are defined below.

Tension test:

$$\sigma_{\text{eff}} = \sigma_{11} = \frac{P}{A} \quad \text{and} \quad \varepsilon_{\text{eff}} = \varepsilon_{11} = \text{Ln}\,\frac{(l+e)}{l}$$

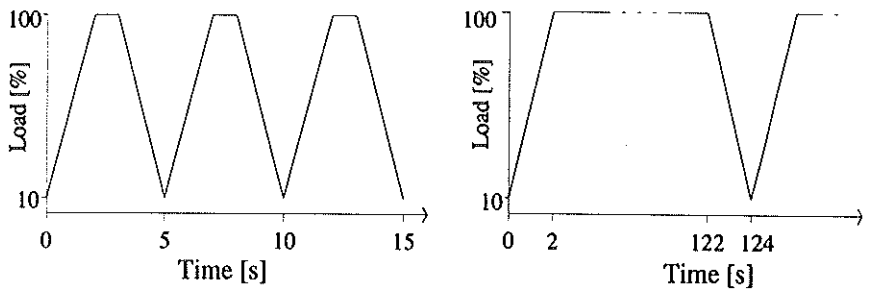


**Fig 3 Cyclic and dwell loading waveforms.**

Torsion test

$$\sigma_{\text{eff}} = \sqrt{3}\sigma_{21} = \sqrt{3}\,\frac{3T}{2\pi(r_0^3 - r_i^3)} \quad \text{and} \quad \varepsilon_{\text{eff}} = \frac{1}{\sqrt{3}}\,\varepsilon_{21} = \frac{1}{\sqrt{3}}\,\frac{(r_0 + r_i)}{2}\,\frac{\theta}{l}$$

Combined tension and torsion

$$\sigma_{\text{eff}} = \sqrt{(\sigma_{11})^2 + 3(\sigma_{21})^2}$$

where $\sigma_{\text{eff}}$ is effective stress, $\varepsilon_{\text{eff}}$ is effective strain, $\sigma_{11}/\varepsilon_{11}$ and $\sigma_{21}/\varepsilon_{21}$ the tensile and shear stress–strain components respectively, $P$ is load, $A$ is cross-sectional area, $T$ is torque, $r_0$ and $r_i$ the outer and inner gauge radii, and $l$ is the gauge length. For the construction of fatigue life curves, failure under tension was taken as complete specimen separation but under torsion a theta creep analysis (2) of strain–time records allowed a 'life to the onset of tertiary deformation' to be defined.

## 3 Results

### 3.1 *Stress–strain behaviour*

Monotonic true stress versus true strain curves as measured under tension and torsion loading for both IMI834 and basketweave IMI685 are presented in Fig. 4. Application of the modified von Mises criteria clearly gives good correlation between the two loading modes for both materials. (N.B. machine capacity was insufficient to promote failure in either of the torsion tests.)

### 3.2 *Fatigue response*

The cyclic fatigue response of both materials is summarized in Fig. 5. On an effective stress basis, the IMI834 alloy displays a clear dependence on loading mode in which tension loads are more damaging than torsion. Combined tension–torsion testing gives fatigue life values that lie between these two

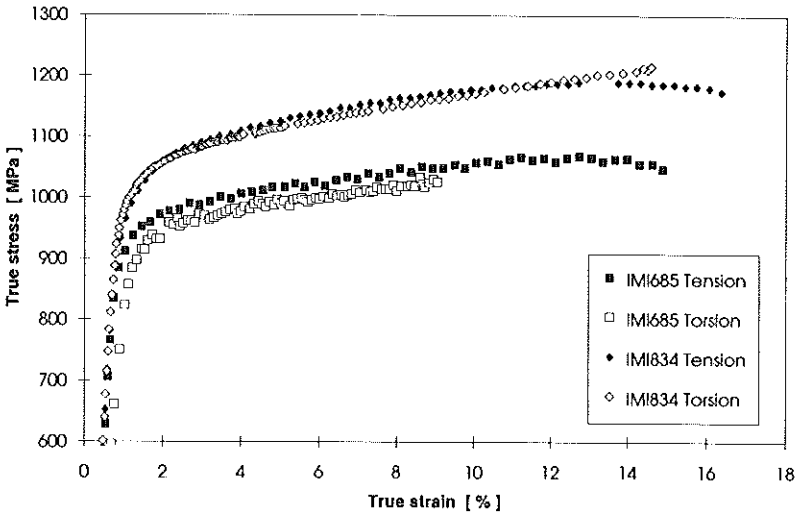


**Fig 4 Monotonic loading curves for IMI685 and IMI834 under tension and torsion.**

extremes. In the case of IMI685, however, the tension life appears to lie within the general scatter band of the torsion data.

The effect of dwell periods at peak stress on fatigue performance is shown for the two alloys in Figs 6 and 7. Figure 6 summarizes behaviour in IMI685. It appears that under torsion, dwell does not influence the fatigue response. For tension, however, a dwell at maximum stress significantly reduces the cyclic life. For reference, a scatter band from previous work on IMI685 with an aligned microstructure has been drawn on the graph. It is evident that the dwell failures largely fall within this band which encompasses aligned tubular and solid specimen test results. One point of additional interest on this graph is the dashed line drawn through the cyclic tension data. It is possible that the tension results have a slightly different slope and this is considered in the discussion. In the case of IMI834, the more limited data suggest that dwell does not affect torsion response but that there is an effect under tension. This tension dwell sensitivity, however, is comparatively small compared with IMI685.

### 3.3 *Fractography*

Failures in basketweave IMI685 can be categorized in a similar way to that reported previously, for the aligned microstructure (1). Effectively there are two categories according to the magnitude of applied stress. At high stresses/strains features consistent with shear deformation are dominant. Under tensile load slip-bands are evident on the specimen gauge surface and inclined facets on the fracture surface produce 'rooftop' effects (1). Under torsion, flat shear failures

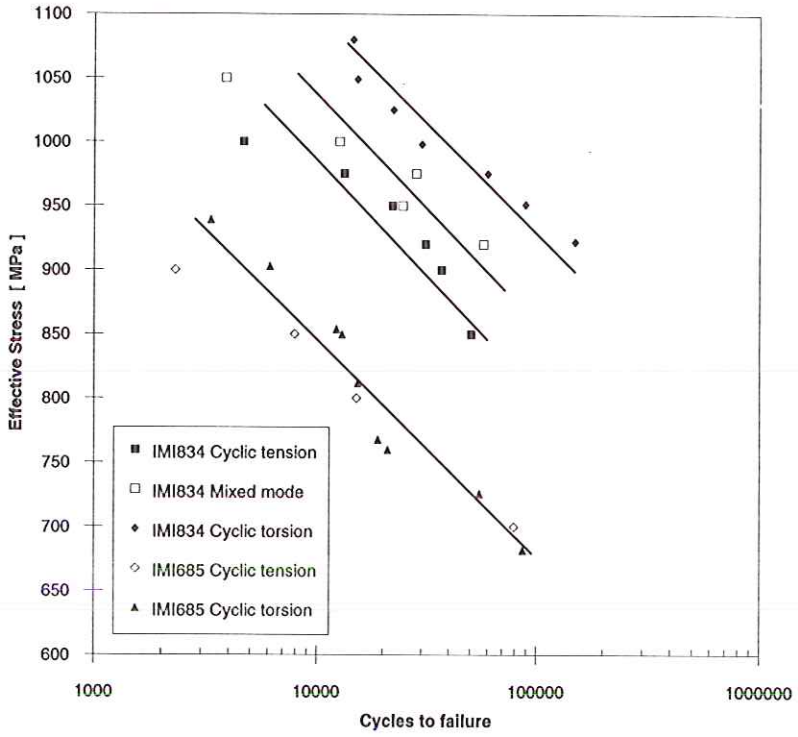


**Fig 5 Cyclic fatigue response of IMI685 and IMI834 under various cyclic stressing modes.**

occur which are largely featureless due to abrasion on the fracture plane. At low stress levels, less than monotonic yield, both tension and torsion specimens demonstrate an increasing influence of tensile stress. The torsion failures become more helical in form with the cracks propagating perpendicular to the maximum principal stress. The IMI834 alloy also displays a greater tendency for helical fractures at low stress but there are important differences. With IMI685 there is a tendency for the helices to be made up of interlinking longitudinal and transverse shear regions. In IMI834, the fracture path is more typical of Stage II fatigue crack growth.

Tension failures in IMI685, are characterized by the presence of quasicleavage facets. In the case of the cyclic fractures, the facets are inclined and situated close to the inner or outer surfaces of the tubular specimen. Under dwell, the extent of the faceting increases and, most noticeably, there is a greater tendency for them to be aligned virtually perpendicular to the tensile stress axis. A typical facet is shown in Fig. 8(a). A characteristic of all facets was the good definition of features on their surface suggesting that there had been little contact during the fatigue life.

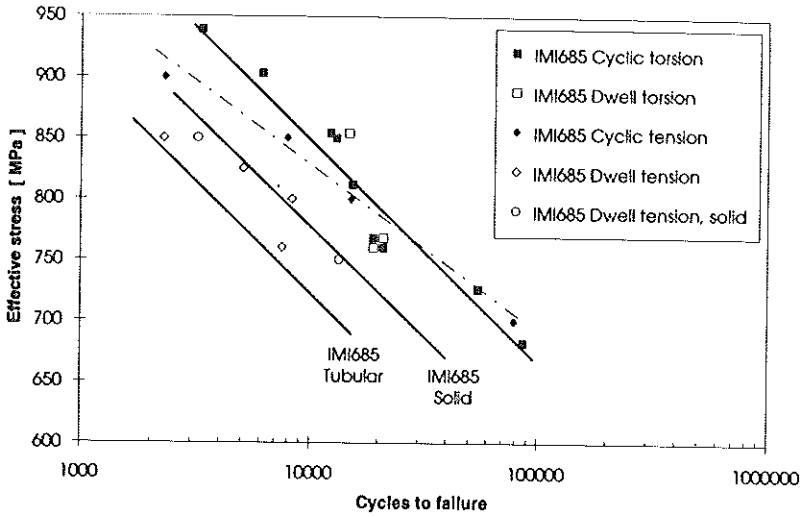


Fig 6 The effect of dwell loading on IMI685.

Faceting was also observed in tension on IMI834 failures but these facets were considerably smaller than in the case of IMI685. Typically they were comparable in size to the alloy grain size, Fig. 8(b). The facets, however, constituted only a small part of the overall fatigue crack region. The majority of the area was made up of Stage II, striation-dominated crack growth, Fig. 8(c).

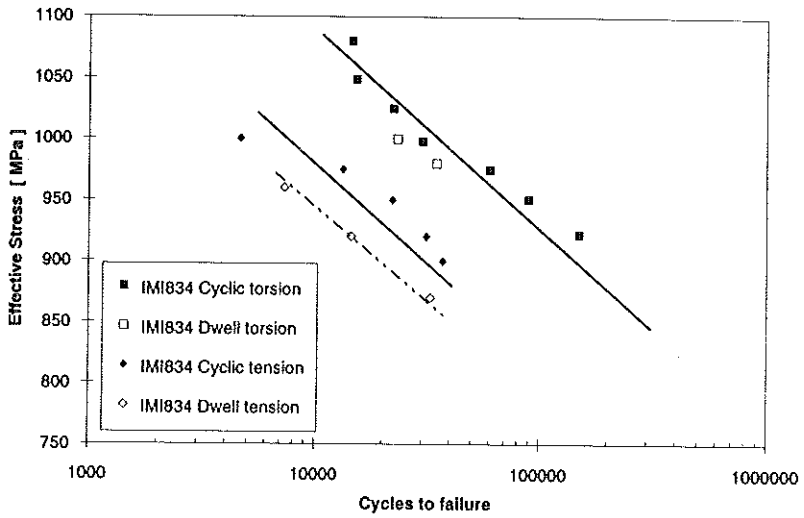


Fig 7 The effect of dwell loading on IMI834.

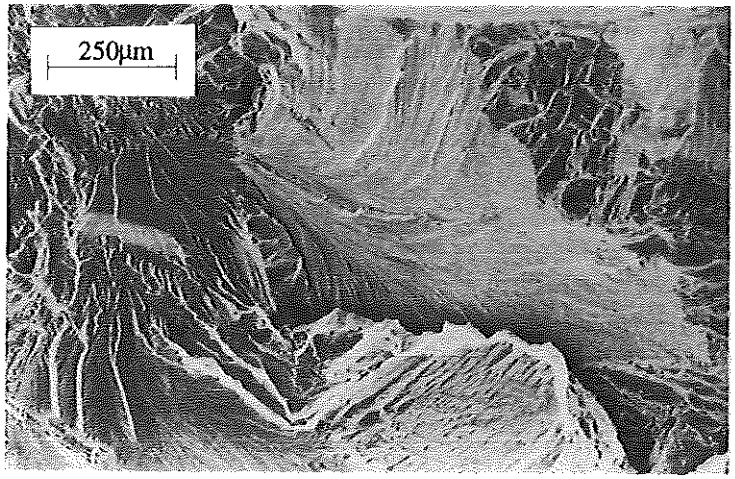


Fig 8(a) Inclined facet in IMI685 under cyclic tension.

## 4 Discussion

There are some similarities but important differences between the two titanium alloys, IMI685 and IMI834, in their response to tension and torsion cyclic loading and in their reaction to dwell periods at peak stress. These factors can be related to the widely different microstructures, both in terms of scale and

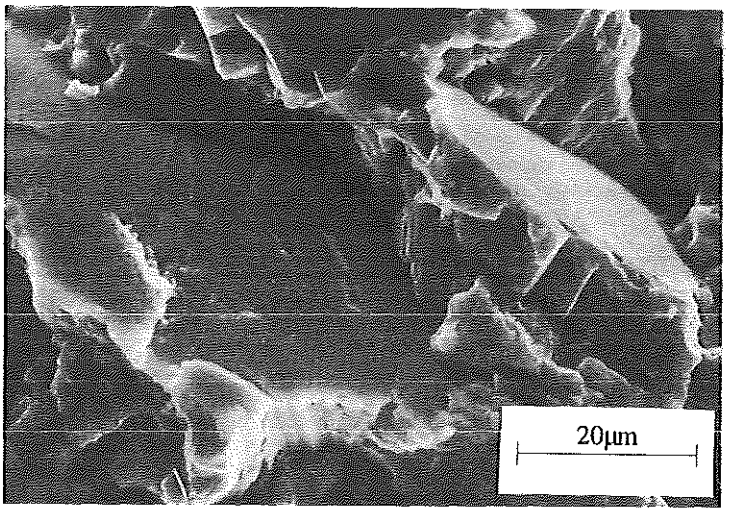


Fig 8(b) Inclined facetting in IMI834 under cyclic tension.

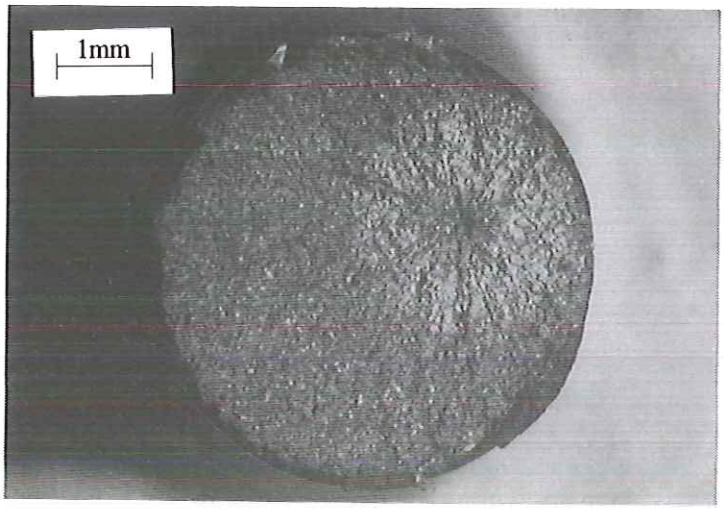


**Fig 8(c) Stage II crack growth from sub-surface initiation site in IMI834.**

morphology, and to the relative importance of crack development events in the two alloys. Interpretation of the observations leads to some important deductions about fatigue crack evolution in this important class of materials.

It is well established that quasicleavage facet formation is an integral part of the early stages of fatigue crack development in the near-alpha and alpha-beta titanium alloys (**3–5**). The present work is consistent with that view as the fracture surfaces for IMI685 and IMI834, Figs 8(a) and (b) demonstrate. The facets are associated with planar slip (**4**) and have been shown to have a basal or near-basal plane orientation (**6**). Wojcik, Chan and Koss (**5**) have demonstrated how the (0001) slip bands progressively decohere. They point out that, in addition to the shear process, a tensile stress normal to the slip plane is an essential requirement. This is consistent with a large number of biaxial fatigue studies which show that, for Stage I cracks, damage models need to include both shear stresses or strains and normal stresses on planes of maximum shear (**7**).

The IMI685 has a relatively coarse microstructure with a prior beta grain size of about 0.5 mm. The heat treatment aims to produce a basketweave structural form but almost inevitably within this general morphology there will be regions in which the alpha phase is aligned. It is believed that the aligned structure is inferior and may be associated with the occurrence of low fatigue life values and facet formation in the alloy. A detailed study of IMI685 with an aligned microstructure and its performance under cyclic and dwell fatigue is the subject of a separate paper (**8**).

Focusing first on IMI685, it is evident that the fatigue response is characterized by the presence of quasicleavage facets and is dominated by initiation and

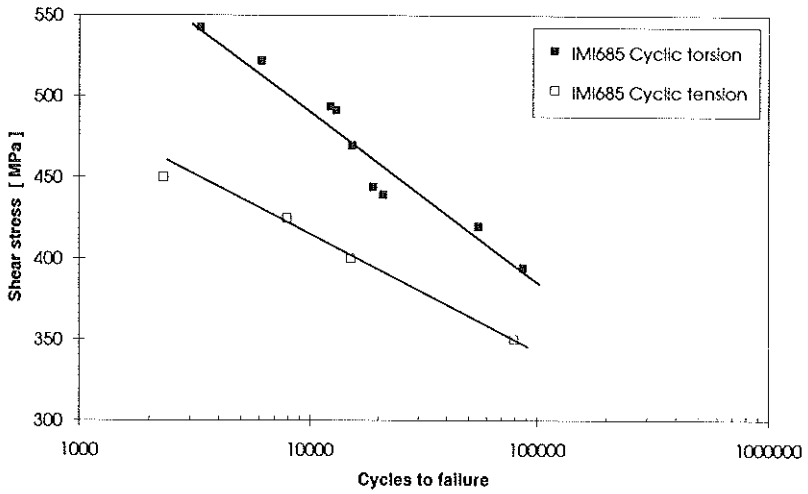


**Fig 9 Cyclic fatigue data for IMI685 plotted on a shear stress basis.**

structure-dominated short-crack growth. The microstructural unit size in relation to the wall thickness of the tubular specimen implies that failure occurs after the crack has traversed a small number of grains. It is evident from Fig. 6 that cyclic tension and torsion data correlate when expressed in terms of the modified effective stress. This correlation is dependent on the assumption that the thin wall has completely yielded. This can be justified on the grounds of the small number of prior beta grains across the section and the fact that there are significant levels of strain accumulation at the stress levels evaluated. The effectiveness of this approach is confirmed by the observed correlation between effective stress–strain loading curves under monotonic tension and torsion, Fig. 4. The significance of a similar effective stress correlation for the fatigue data is not clear at present but might imply the need to cater for an 'averaged shear stress' in a material with highly anisotropic slip characteristics (9).

When the cyclic data are plotted on a maximum shear stress basis, the tension tests have significantly lower lives for a given $\tau_{max}$, Fig. 9. Furthermore, the trend pointed out by the dashed line in Fig. 6, i.e. a greater tensile influence at high stress, is reinforced by this format. These observations are consistent with other biaxial fatigue studies and are taken to imply that crack development is enhanced by the presence of a stress normal to the plane of growth. The fracture surface studies demonstrate that the cyclic tension failures are associated with facets inclined at approximately 45° to the loading axis and adjacent to either the inner or outer wall of the tube. A typical example is shown in Fig. 8(a). These facets are comparatively small compared to those found previously on aligned material (8). Their clean appearance suggests that separation has

occurred with little contact or rubbing of the surface, presumably due to a resolved tensile stress on the plane of shear. The facets in fact are similar to those observed by Wojcik *el al.* in their studies of Stage I crack growth at slip bands (**5**). In torsion the fractures tend to be 'shear dominated' at the higher stresses but to have a 'helical' morphology at lower stresses. Even so, a number of these macroscopic helical crack paths appeared to be comprised of consecutive regions of microscopic transverse and longitudinal shear. Tensile and shear processes, therefore, also play a part in the growth of the cracks in torsion although the smaller contribution of the normal stress was evident in the extensive surface contact on the planes of shear.

When a period of dwell at peak stress is imposed on the fatigue cycle, there is a marked change in the way the IMI685 alloy responds to tension and torsion loading. For both loading modes there is an increase in strain accumulation during the fatigue test. In the torsion case, this is associated with a greater contribution from shear to the failure process even when the overall crack growth mode is helical. However, with torsion there is little or no effect on the cyclic life, Fig. 6. In contrast, the tension cyclic lives are reduced significantly by the dwell periods. The fractures also display some significant changes. In particular, facets are more perpendicular to the stress axis and tend to be very large, virtually traversing the full wall thickness in some cases. This change in fracture mode has been attributed to the formation of hydrides (**11**). However, recent work by the authors (**8**) demonstrates that similar features form, even when the hydrogen level is reduced to less than 20 ppm. Furthermore, they also occur in thin, plane stress sections. Moody and Gerberich have shown that hydride formation is difficult under these conditions (**12**).

An alternative mechanism for the formation of these 'perpendicular' facets has been suggested. It is recognized that slip under shear is essential and that a stress normal to the slip plane is an advantage in the formation of the facets. It is also known that the facets form on basal planes. Basal planes that are virtually perpendicular to the stress axis have the advantage of a large normal stress but the disadvantage of an orientation that is difficult for slip. Therefore, it is argued that slip will occur in adjacent and more favourably positioned grains. Through the Stroh pile-up model (**13**), it can be shown that the required shear stress is able to develop on near-perpendicular basal planes. Furthermore, a tensile stress additional to the existing normal stress will be generated. Strain accumulation, therefore, promotes the formation of these large perpendicular facets.

The model was developed to account for dwell and cyclic failures in the fully aligned microstructure. It is significant that the tensile dwell failures in the basketweave microstructure coincide with the band defined for cyclic and dwell fatigue life behaviour in aligned material (Fig. 6). It has already been stated that the basketweave heat treatment results in some aligned regions. It is argued that the resultant low dwell lives are due to crack formation within aligned enclaves that are appropriately orientated.

The IMI834 alloy has a much finer microstructure than IMI685. It consists of 15% primary alpha phase in a transformed beta matrix, with typical grain dimensions of 20–30 $\mu$ms. In this case, the cyclic fatigue response displays a strong dependence on loading mode even when the data are expressed in terms of effective stress. It is clear from Fig. 7 that cyclic life is significantly reduced by a tensile stress component. It is argued that this different response from IMI685 is due to the fact that a different stage of the crack development process dominates the fracture process. Examination of the fracture surfaces strongly suggest that striation-dominated stage II crack growth is prevalent.

Figure 8(c) shows that there is a tendency for subsurface crack formation under tension. In a region near the centre of the crack is a small zone of quasicleavage facets, Fig. 8(b). Outside this zone striation-based crack growth is evident. Under torsion, the fracture path is essentially helical without an obvious tendency for sub-division into transverse and longitudinal shear regions. This type of growth is again typical of Stage II crack development under a maximum principal stress. The fact that this normal stress is smaller in torsion than tension can be related to the longer cycle lives obtained under this mode. For dwell conditions, the limited data available suggest that there is no effect in torsion and only a small reduction in life under tension. In-house studies have shown that dwell periods have no influence on room temperature Stage II crack growth in these materials. The small effect in tension, therefore, can be attributed to earliest stages of crack development when quasicleavage facets are forming in a similar way to that already discussed for IMI685.

## 5 Conclusions

The paper has defined clear differences between the titanium alloys IMI685 and IMI834 in terms of their response to tension and torsion loading and to the imposition of dwell periods at peak stress. These differences can be attributed to the scale of the microstructure in each alloy and to the fact that the cracks are growing in a structurally sensitive or small crack mode in IMI685 but are predominantly Stage II in IMI834. The following can be stated.

(1) On an effective stress basis, there is little difference between cyclic tension and torsion failure cycle lives in IMI685.
(2) A dwell period significantly reduces cyclic tension life in IMI685 probably because of aligned microstructural features within the general basketweave matrix. However, there is little impact in torsion highlighting the need for a tensile stress on active shear planes.
(3) On an effective stress basis, tension gives a significantly shorter cyclic life than torsion in IMI834. Mixed mode tension/torsion loading results in an intermediate fatigue life behaviour.
(4) Dwell has no effect on torsion behaviour in IMI834 but reduces tension life cycle by an amount that is significantly less than in the case of the IMI685 alloy.

## References

(1) BACHE, M. R. and EVANS, W. J. (1992) Tension and torsion fatigue testing of a near alpha titanium alloy, *Int. J. Fatigue*, **14**, pp. 331–337.
(2) EVANS, R. W. and WILSHIRE, B. (1985) *Creep of Metals and Alloys*, Institute of Metals, London.
(3) EVANS, W. J. (1987) Stress relaxation and notch fatigue in Ti–6Al–4V, *Scripta Met.*, **21**, pp. 1223–1227.
(4) SONG, Z. and HOEPPNER, D. W. (1989) Size effect on the fatigue behaviour of IMI829 titanium alloy under dwell conditions, *Int. J. Fatigue*, **11**, (2), pp. 85–90.
(5) WOJCIK, C. C., CHAN, K. S. and KOSS, D. A. (1988) Stage I fatigue crack propagation in a titanium alloy, *Acta Met.*, **36**, pp. 1261–1270.
(6) DAVIDSON, D. L. and EYLON, D. (1980) Titanium alloy fatigue fracture facet investigation by selected area electron channelling, *Met. Trans. A*, **11A**, 837–843.
(7) SOCIE, D. F. (1993) A critical plane approach for multiaxial fatigue damage assessment, *Advances in Multiaxial Fatigue*, **ASTM STP 1151**, (edited by D. L. McDowell and R. Ellis,) pp. 7–36.
(8) EVANS, W. J. and BACHE, M. R. (1994) Dwell sensitive fatigue under biaxial loads in the near alpha titanium alloy IMI685, *Int. J. Fatigue*, **16**, pp. 443–452.
(9) DIETER, G. E. (1988) *Mechanical metallurgy*, McGraw-Hill Book Company, p.79.
(10) McDIARMID, D. L. (1989) Crack systems in multiaxial fatigue, *Proc. Seventh Int. Conf. on Fracture*, (Edited by K. Salama *et al.*) Pergamon, pp. 1265–1277.
(11) HACK, J. E. and LEVERANT, G. R. (1982) The influence of microstructure on the susceptibility of titanium alloys to internal hydrogen embrittlement, *Met. Trans. A*, **13A**, pp. 1729–1738.
(12) MOODY, N. R. and GERBERICH, W. W. (1982) The effect of stress state on internal hydrogen-induced crack growth Ti–6Al–6V–2Sn, *Met. Trans. A*, **13A**, pp. 1055–1061.
(13) STROH, A. N. (1954) The formation of cracks as a result of plastic flow, *Proc. Roy. Soc. (London)*, **223**, pp. 404–414.